

# Retrieval of Land-surface Temperature from AMSR2 Data Using a Deep Dynamic Learning Neural Network

MAO Kebiao<sup>1,2,3</sup>, ZUO Zhiyuan<sup>1</sup>, SHEN Xinyi<sup>4</sup>, XU Tongren<sup>2</sup>, GAO Chunyu<sup>1</sup>, LIU Guang<sup>3</sup>

(1. National Hulunber Grassland Ecosystem Observation and Research Station, Institute of Agricultural Resources and Regional Planning, Chinese Academy of Agricultural Sciences, Beijing 100081, China; 2. State Key Laboratory of Remote Sensing Science, Institute of Remote sensing and Digital Earth Research, Chinese Academy of Science and Beijing Normal University, Beijing 100086, China; 3. College of Resources and Environments, Hunan Agricultural University, Changsha 410128, China; 4. Hydrometeorology and Remote Sensing Laboratory, University of Oklahoma, Norman 73072, USA)

**Abstract:** It is more difficult to retrieve land surface temperature (LST) from passive microwave remote sensing data than from thermal remote sensing data, because the emissivities in the passive microwave band can change more easily than those in the thermal infrared band. Thus, it is very difficult to build a stable relationship. Passive microwave band emissivities are greatly influenced by the soil moisture, which varies with time. This makes it difficult to develop a general physical algorithm. This paper proposes a method to utilize multiple-satellite, sensors and resolution coupled with a deep dynamic learning neural network to retrieve the land surface temperature from images acquired by the Advanced Microwave Scanning Radiometer 2 (AMSR2), a sensor that is similar to the Advanced Microwave Scanning Radiometer Earth Observing System (AMSR-E). The AMSR-E and MODIS sensors are located aboard the Aqua satellite. The MODIS LST product is used as the ground truth data to overcome the difficulties in obtaining large scale land surface temperature data. The mean and standard deviation of the retrieval error are approximately 1.4° and 1.9° when five frequencies (ten channels, 10.7, 18.7, 23.8, 36.5, 89 V/H GHz) are used. This method can effectively eliminate the influences of the soil moisture, roughness, atmosphere and various other factors. An analysis of the application of this method to the retrieval of land surface temperature from AMSR2 data indicates that the method is feasible. The accuracy is approximately 1.8° through a comparison between the retrieval results with ground measurement data from meteorological stations.

**Keywords:** radiometry; Advanced Microwave Scanning Radiometer 2 (AMSR2); passive remote sensing; inverse problem

**Citation:** MAO Kebiao, ZUO Zhiyuan, SHEN Xinyi, XU Tongren, GAO Chunyu, LIU Guang, 2018. Retrieval of Land Surface Temperature from AMSR2 Data Using a Deep Dynamic Learning Neural Network. *Chinese Geographical Science*, 28(1): 1–11. <https://doi.org/10.1007/s11769-018-0930-1>

## 1 Introduction

The extensive requirement of large scale temperature information for climate change and agricultural research has made the remote sensing of the land surface temperature (LST) an important issue during recent decades. Passive microwave data and thermal infrared data have their own advantages and disadvantages. Thermal

infrared remote sensing data have a high resolution, but they are greatly influenced by clouds. Passive microwave data are affected relatively little by clouds, while their resolution is relatively low. Therefore, making full use of their respective advantages has become a research hotspot.

Many algorithms (Price, 1984; Becker and Li, 1990; Sobrino et al., 1991; Kerr et al., 1992; Coll et al.,

Received date: 2017-07-20; accepted date: 2017-11-07

Foundation item: Under the auspices of National Natural Science Foundation of China (No. 41571427), National Key Project of China (No. 2016YFC0500203), Open Fund of State Key Laboratory of Remote Sensing Science (No. OFSLRSS 201515)

Corresponding author: MAO Kebiao. E-mail: maokebiao@caas.cn

© Science Press, Northeast Institute of Geography and Agroecology, CAS and Springer-Verlag GmbH Germany, part of Springer Nature 2018

1994; Prata, 1994; Wan and Dozier, 1996; Gillespie, 1998; Liang, 2001; Mao et al., 2005, 2007a, 2008, Chen et al., 2011; Xia et al., 2014) have been proposed to retrieve sea/land surface temperature from thermal data, including MODIS, and AVHRR data. The accuracies of most such algorithms are very high, but thermal remote sensing is influenced greatly by clouds, atmospheric water vapor content and rainfall. Over 50% of the area in MODIS LST product is influenced by clouds and rainfall (Mao et al., 2007b). Microwave remote sensing has the advantage in these respects because it can overcome the shortcomings of thermal remote sensing, such as the sensitivity to cloud cover, smoke, and aerosol effects.

Although many studies (Susskind et al., 1984; McFarland et al., 1990; Choudhury et al., 1992; Kerr and Njoku, 1993; Calvet et al., 1994; Calvet et al., 1996; Givri, 1997; Pulliainen et al., 1997; Basist et al., 1998; Weng and Grody, 1998; Aires et al., 2001; Morland et al., 2001; Dash et al., 2002; Fily et al., 2003; Prigent et al., 2003; Mao et al., 2007b; 2007c) have shown that passive microwave data could be used to estimate the surface temperature without prior knowledge of the emissivity, absorption, or scattering for known surface conditions, land surface temperature retrieval from passive microwave has not been widely used in application. Most methods used to retrieve the land surface temperature distribution from passive microwave data are empirical and local, because passive microwave observations are sensitive to the soil moisture (Owe et al., 2001; Njoku et al., 2003), vegetation structure and biomass (Jackson et al., 1982; Paloscia and Pampaloni, 1988; Jackson and O'Neill, 1990; Jackson and Schmugge, 1991; Jackson, 1997; Njoku and Chan, 2006). However, the radiative mechanisms of snow and frozen ground are different from those of bare soil and vegetation (McFarland et al., 1990). The biggest difficulty is obtaining large scale ground truth measurements of LST that match those in the large scale pixels (generally exceeding 25 km by 25 km) of passive microwave data from the satellite pass to develop and validate the algorithm (Mao et al., 2007c). Ground measurements are generally point measurements, and thus, utilizing multiple sensor instruments and multiple resolution characteristics is an important task in remote sensing. In most previous studies, the skin temperature was mainly obtained from infrared radiometer or meteorological

measurements (i.e., the air temperature at 1–2 m above the ground) (Susskind et al., 1984; McFarland et al., 1990; Choudhury et al., 1992; Kerr and Njoku, 1993; Calvet et al., 1994; Calvet et al., 1996; Givri, 1997; Pulliainen et al., 1997; Basist et al., 1998; Weng and Grody, 1998; Aires et al., 2001; Morland et al., 2001; Dash et al., 2002; Fily et al., 2003; Prigent et al., 2003; Mao et al., 2007b; 2007c). Sensors such as the AVHRR provide a good spatial resolution with a limited sampling time, while the TIR sensors on board geostationary weather satellites offer adequate sampling but with poorer spatial resolutions (Prigent et al., 2003). Some researchers used data sets produced by the International Satellite Cloud Climatology Project (ISCCP), but their resolution is also very low (approximately 30 km by 30 km) (Aires et al., 2001). Alternatively, the two EOS (Earth Observing System) AMSR-E and MODIS sensors are equipped on the Aqua satellite. AMSR-E is a passive microwave radiometer that observes atmospheric, land, oceanic, and cryospheric parameters, including precipitation, sea surface temperature, ice concentration, snow water equivalent, surface wetness, wind speed, atmospheric cloud water, and water vapor content data. The AMSR-E Level 2A product (AE\_L2A) contains brightness temperature (TB) data at 6.9, 10.7, 18.7, 23.8, 36.5, and 89.0 GHz that are resampled to be spatially consistent, and it is available at a variety of resolutions that correspond to the footprint sizes of the observations (56, 38, 24, 21, 12, and 5.4 km, respectively). MODIS has 36 bands which are designed for retrievals of sea surface temperature (SST), land surface temperature (LST) and atmospheric properties. The resolution of MODIS ranges from 250 m to 1000 m. The two instruments can complement one another. The MODIS sensor has a high resolution, but it is influenced greatly by clouds. The algorithms used to retrieve the land surface temperature from MODIS data are mature, and NASA has provided land surface temperature products, with accuracies of approximately 1 K on clear days (Wan et al., 2002, 2004). However, the AMSR-E antenna stopped spinning in late 2011, and AMSR-E data do not exist after this date. Fortunately, a similar sensor, the Advanced Microwave Scanning Radiometer 2 (AMSR2) has been onboard the GCOM-W1 satellite since 2012. The AMSR2 Level 1 product contains brightness temperature (TB) data at 6.9 GHz, 7.3 GHz, 10.7 GHz, 18.7 GHz, 23.8 GHz, 36.5 GHz, and 89.0 GHz. The AMSR2

GHz. The AMSR2 sensor exhibits a new frequency (7.3 GHz), while the other frequencies are the same as those contained within the AMSR-E sensor, and thus, it provides a chance to utilize multiple-satellite/sensor/ resolution to retrieve land surface temperature from passive microwave data.

In order to improve estimation accuracy from passive microwave data, we first analyze the ill-posed problem and potential information characterized by different parameters, after which we use a deep learning dynamic neural network to retrieve LST from AMSR2 data. The training and testing data are obtained from MODIS and AMSR-E data. The MODIS LST product is used as the large scale land surface data to overcome the difficulty encountered in obtaining large scale ground truth LST measurements that match those at the pixel scale of passive microwave AMSR-E data from the satellite pass.

## 2 Data and Methods

### 2.1 Data

The overall method and routine of this research can be described using a flow map as shown in Fig. 1. We initially analyze the currently employed algorithms, and

select the deep dynamic learning neural network algorithm proposed by Tzeng et al. (1994) as the base for the algorithm. The key to the accuracy of a neural network is the method used to obtain the high-precision training and testing data. It is very difficult to obtain in situ ground truth LST measurements that match those at the pixel scale (24 km by 24 km at nadir) of AMSR2 data during the satellite pass for the training and testing data for the algorithm. Generally, the LST varies from point to point, and ground measurements are generally point measurements. Therefore, it is difficult to obtain LST measurements that match those in the pixels of AMSR2 data. Additionally, the AMSR2 sensors observe the ground at different angles, and thus, it is also difficult to precisely locate the pixel of the measured ground in AMSR2 data, especially within nighttime images. The AMSR2 data share similar characteristics with those of Advanced Microwave Scanning Radiometer for EOS (AMSR-E). The AMSR-E and MODIS sensors are located on the Aqua satellite. MODIS LST products can be used as ground truth data to overcome the difficulty in obtaining large scale land surface temperature data. The AMSR-E bright-temperature data (10.7 V/H, 18.7 V/H, 23.8 V/H, 36.5 V/H, 89 V/H GHz) and the corresponding MODIS surface temperature data can be used

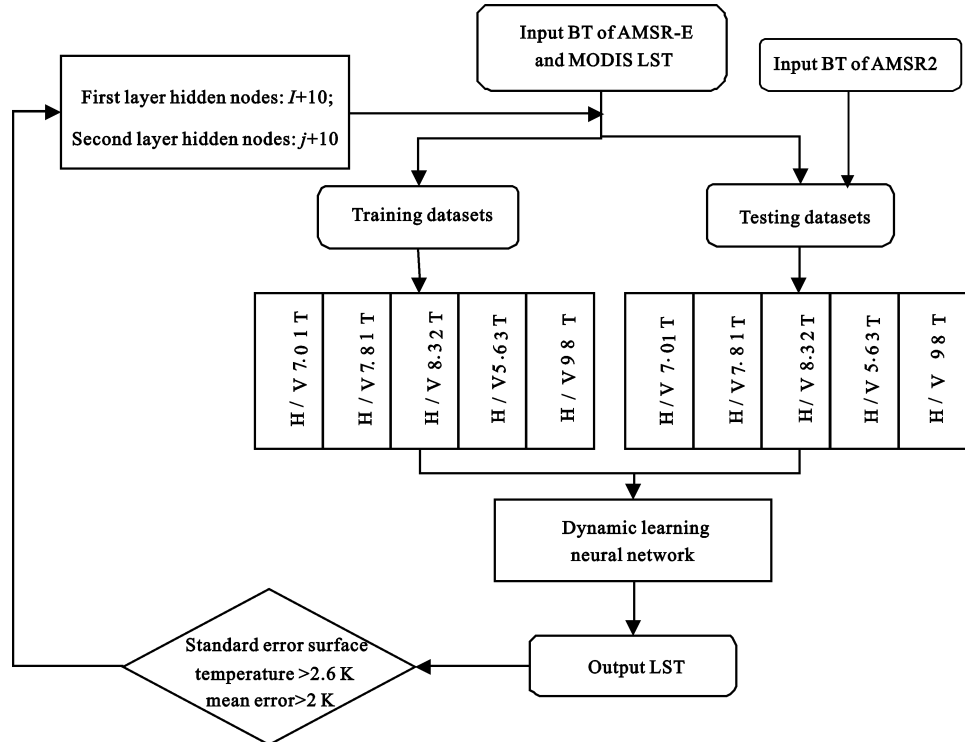


**Fig. 1** Flow map of the retrieval LST from AMSR-E/AMSR2 data

as the training and testing data for the dynamic learning neural network algorithm. Then, after the neural network is trained, the AMSR2 bright temperature data are used as input data to estimate the surface temperature.

## 2.2 Microwave radiation transmission theory

A microwave radiometer measures the thermal emission of the ground and its transfer from the ground through the atmosphere to the remote sensor on the satellite. According to the Rayleigh-Jeans approximation for the Planck function, the radiation intensity observed by the radiometer can be written simply as expression (1) (Kerr and Njoku, 1990).

$$\begin{aligned} T_{bp}(\tau, \mu) = & (1 - \omega)(1 - e^{-\tau})[1 + (1 - \varepsilon_p)e^{-\tau}]T_c + \\ & \varepsilon_p T_s e^{-\tau} + t(1-t)(1 - \varepsilon_p)T_a^\downarrow + (1-t)T_a^\uparrow \end{aligned} \quad (1)$$

where  $P$  represents the horizontal (H) or vertical (V) polarization,  $\varepsilon_p$  is the emissivity,  $\tau$  (the equivalent canopy optical depth) and  $\omega$  (the single scattering albedo) are two important parameters that characterize the absorbing and scattering properties of the vegetation,  $T_s$  is the land surface temperature,  $T_c$  is the average temperature of the vegetation,  $T_{bp}(\tau, \mu)$  is brightness temperature of the radiation emitted by the canopy at an angle  $\theta$ ,  $t$  is the transmittance of the atmosphere,  $T_a^\uparrow$  is the upwelling average atmosphere temperature, and  $T_a^\downarrow$  is the downwelling average atmospheric temperature. Centimeter wave bands are influenced little by the atmosphere, and the transmittance ( $t$ ) of a microwave is very high (approximately equal to 1) even when the water vapor content is approximately  $5 \text{ g/cm}^2$  in the atmosphere (Njoku et al., 1999) in low frequency bands. Thus, the influence of the atmosphere is very little, and equation (1) can be simplified into equation (2).

$$T_{bp}(\tau, \mu) = (1 - \omega)(1 - e^{-\tau})[1 + (1 - \varepsilon_p)e^{-\tau}]T_c + \varepsilon_p T_s e^{-\tau/\mu} \quad (2)$$

$T_c$  is usually assumed to be equal to  $T_s$  when the soil is covered by vegetation (Njoku et al., 2003; Paloscia and Pampaloni, 1988). The parameter  $\tau$  (the canopy opacity) is a function of the vegetation water content ( $w$ ), the view angle ( $\theta$ ), and the constant  $b$  (Njoku and Li., 1999).

Based on equations (1) and (2), it is very difficult to retrieve the land surface temperature from passive microwave remote sensing data because a single frequency

thermal measurement involves at least two unknowns (the emissivity and LST), which constitutes a typical ill-posed inversion problem. However, the emissivity is mainly influenced by dielectric constant which is a function of the physical temperature, salinity, water content, soil texture and other factors (e.g., vegetation) (Dobson et al., 1985; Hallikainen et al., 1985). The soil moisture, roughness and land surface temperature vary with the weather, and time making the retrieval more complicated because different combinations of the soil moisture, roughness and land surface temperature can provide the same emissivity.

The geophysical parameters are not independent from one another. In our previous research, we did not make full use of the relationship between them in land surface temperature retrieval methods (Mao et al. 2007a). In fact, a relationship between different geophysical parameters was proved through simulation analysis by using AIEM and Qp mode (Shi et al., 2005). A comparison of different emissivity simulations by using the Qp model and the AIEM indicated that the absolute error is extremely small with a magnitude of  $10^{-3}$  (Shi et al., 2005). Fily et al. (2003) found that the emissivities ( $\varepsilon$ ) in the V and H polarization are linearly related by the empirical parameters A and B in dry region at high latitudes.

$$\varepsilon_v = A\varepsilon_h + B \quad (3)$$

We use the AIEM (Chen et al., 2003; Wu et al., 2001) to generate simulation data, and then use a dynamic learning neural network (DL) (Tzeng et al., 1994) to conduct a retrieval analysis. The retrieval analysis indicates that a neural network can be used to accurately retrieve soil moisture and land surface temperature from passive microwave data. The mean and the standard deviation of the retrieval error are less than 2 K. The simulation data from the theoretical model contain some limitation in real applications because the data do not consider the terrain and the structure of the vegetation. Most pixels in AMSR passive microwave data are mixed at coarse spatial resolutions (24 km by 24 km). A real signal is a more complex than the signal simulated using a theoretical model. It is very difficult to simulate a hybrid signal at a large scale using the general physical model. Fortunately, MODIS land surface temperature products provide data to match the large scale land surface measurement data from AMSR-E. Furthermore, a neural network with only a single hidden layer con-

taining a sufficient number of nodes with a nonlinear activation function can approximate any continuous scalar function under a given precision in a finite domain (Hornik et al., 1989; Blackwell, 2005). Many studies have shown that multiple layer network can be used for classification purposes (Bischof et al., 1992; Herrmann and Khazene, 1992; Tzeng, 1994) and inversion (Chen et al., 1992; Tang et al., 1992; Jin and Lin, 1997; Aires et al., 2001; Faure et al., 2001; Tedesco et al., 2004; Blackwell, 2005; Mao et al., 2007a; 2007c, 2008). Since neural networks simultaneously possess function approximation, classification, optimization computation and self-study capabilities, we can utilize a neural network with MODIS LST data to retrieve land surface temperature from AMSR-E/AMSR2 data.

### 2.3 Analysis of land surface temperature retrieval from AMSR2 data using a neural network

A neural network (NN) may be the best possible choice because it does not require the derivation of rules, and can combine some classification information with optimization computation. We make the MODIS land surface temperature product match the land surface measurements from the AMSR-E data because the two instruments are both located on the Aqua satellite. The MODIS/Aqua land surface temperature/emissivity 5-MIN L2 product (the MOD11\_L2 product with LST in 1 km pixels) provides per-pixel temperature and emissivity values. The temperatures are extracted in kelvin using the generalized split-window algorithm (Wan and Dozier, 1996). The emissivities are derived from land cover database information. On a clear day, the accuracy of the land surface temperature product is very high (under 1K) (Wan et al., 2002; 2004). An AMSR-E pixel includes many MODIS pixels. In practice, the value of a pixel in the MODIS product is 0 when it is covered by clouds or when there is rainfall in the pixel. Equation (4) is used to compute the land surface temperature obtained from the MODIS LST product that matches an AMSR-E pixel, where the average value from all of the MODIS LST pixels is set as the land surface temperature in the AMSR-E pixel.

$$T_{\text{AMSR2}} = \frac{\sum_{i=1}^{N \geq 25} T_{\text{MODIS}}^i}{N} \quad (4)$$

where  $T_{\text{MODIS}}^i$  is the land surface temperature from the

MODIS LST product,  $T_{\text{AMSR2}}$  is the land surface temperature of AMSR-E, and  $N$  is the number of MODIS pixels without the influences of either cloud or rainfall in the AMSR-E pixel. The acquisition process for the training and testing data is shown in Fig. 2.

To make the retrieval method suitable for cloudy conditions, we set the average values of cloud and rain free pixels in the MODIS LST product to the land surface temperature matching the AMSR-E pixel when the number ( $N$ ) of MODIS pixels absent the influences of either clouds or rainfall is greater than 25. We delete the data set that cannot represent the large scale land surface data of AMSR-E during the training and testing of the neural network. This will overcome the difficulty in obtaining the land surface temperature distribution when an AMSR-E pixel is influenced by clouds or other factors (e.g., rainfall). Five regions (Southeast China, West China, Northwest China, North China and Northeast China) are employed as the data collection regions, for the time period spanning January through December of both 2005 and 2006. We collect 19 237 data sets covering most land surface types and range in the temperature, and divide them randomly into two parts. The total number of training data sets is 11 217 sets and the testing data comprises 8020 sets.

To solve the ill-posed retrieval problem, we select the dynamic learning neural network (DL) (Tzeng et al., 1994), which uses the Kalman filtering algorithm to increase the convergence rate in the learning stage and enhance the separation ability for highly nonlinear boundary problems. The initial neural network weights are set as small random numbers between -1 and 1. The Kalman filtering process is a recursive mean square estimation procedure. Each updated estimate of the neural network weight is computed from the previous estimate and the new input data. The weights connected to each output node are updated independently. The DL quickly achieves the required root mean square (rms) error in only a couple of iterations, and the results trained sing the NN are very stable. The rms threshold is often set to  $1 \times 10^{-3}$  with two iteration. The frequency of 6.9 GHz is influenced by radio frequency interference (RFI) near densely populated areas (Njoku et al., 2005). The brightness temperatures of four channels at 10.7, 18.7, 23.8, 36.5 (V/H) GHz are selected as the eight input nodes because they are influenced little by atmospheric effects and clouds, and the land surface temperature is

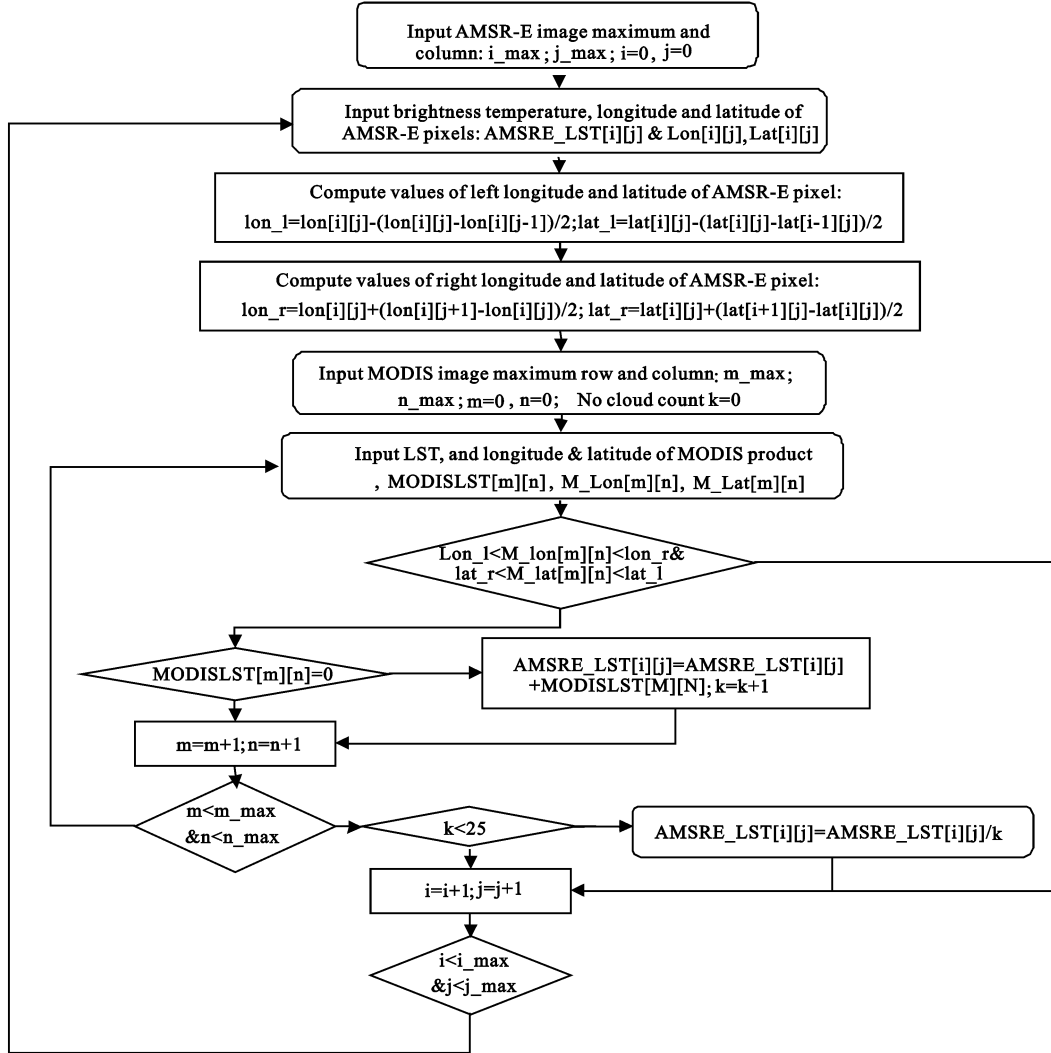


Fig. 2 Flow chart of acquisition of training and testing data

the only output node of the neural network. After trial and error, we set the number of hidden-nodes from small to large, and select the smallest retrieval error for the testing data. Table 1 presents a part of the analysis results. The mean and standard deviation of the retrieval error are approximately  $2.11^\circ$  and  $2.16^\circ$  relative to the MODIS LST product when the number of hidden layers is two and when the number of hidden nodes is 600 in each layer in table1 (second column in table). Although microwave data are advantageous for the retrieval of surface parameters because they are less perturbed by cloud cover than thermal data (Givri, 1997), the influences of the cloud cover and the water vapor content, especially precipitation could not be fully eliminated. The 23.8 GHz, 36.5 GHz and 89 GHz channels can be

used to correct for the atmospheric water vapor content (McFarland et al., 1990; Givri, 1997; Mao et al. 2007b). To improve the retrieval accuracy, we add these high frequencies to eliminate the impacts of the atmosphere, cloud cover and rainfall. A detail summary of the retrieval information is shown in table1 for different combinations of channels. The mean and the standard deviation of the retrieval error are approximately  $1.4^\circ$  and  $1.9^\circ$  relative to the MODIS LST product when five frequencies (ten channels, 10.7, 18.7, 23.8, 36.5, 89 V/H GHz) are combined and when the number of hidden nodes is 500 in each layer. This method can overcome various influences, such as those of the atmosphere, cloud cover, rainfall, roughness, terrain and vegetation distribution).

**Table 1** Summary of the retrieval errors when using different combination of channels

Hidden nodes	10.7, 18.7, 23.8, 36.5 V/H			10.7, 18.7, 23.8, 36.5, 89.0 V/H		
	R	SD	M (°C)	R	SD	M (°C)
100-100	0.980	3.32	2.12	0.991	2.81	2.27
200-200	0.988	2.71	2.2	0.992	2.69	2.18
300-300	0.980	3.41	2.7	0.993	2.67	1.97
400-400	0.970	3.62	2.61	0.993	2.65	1.91
500-500	0.989	2.21	2.12	0.994	1.91	1.39
600-600	0.989	2.16	2.11	0.979	3.71	1.99
700-700	0.983	2.81	2.11	0.988	3.32	1.88
800-800	0.975	3.68	2.33	0.975	3.68	1.94

Notes: R: correlation coefficient; SD: standard deviation of error; M (°C): mean error relative to MODIS LST

### 3 Results and Discussion

To provide an example of the application of the algorithm, we utilize the neural network trained above to retrieve the land surface temperature distribution from an AMSR2 image (2013-04-13) in the most East-China. The retrieval results are shown in Fig. 3. Some pixels values are zero in the AMSR2 image because some lakes and flooding are present in those pixels. The existence of these water bodies was subsequently proven using a terrain map of China. There is also heavy rainfall and snow in some of the pixels. The surface temperature retrieval method for lake/sea surface is very different from soil and vegetation surfaces because their radiative mechanism are very different, which can help identify the lakes in passive microwave pixels. Thus, we must construct different retrieval methods or training databases for pixels that include large lakes, or compensate using more training data including large lakes in the AMSR2 pixels.

An evaluation of the retrieval algorithm used to obtain the measured LST values that match the pixels in the AMSR-E data is not straightforward. Generally, the LST varies from point to point on the ground, and ground measurements are generally point measurements. Ground LST measurements used in this study are obtained from various meteorological stations in China. The AMSR2 data resolution is so large that the required number of meteorological stations is more than 3 within large, mostly uniform regions. Therefore, 38 data sets of the land surface temperature are obtained from the meteorological stations in the most East-China for 2013. We retrieve the land surface temperature distribution from the AMSR2 image. A comparison between the retrieval results and the ground measurements indicates

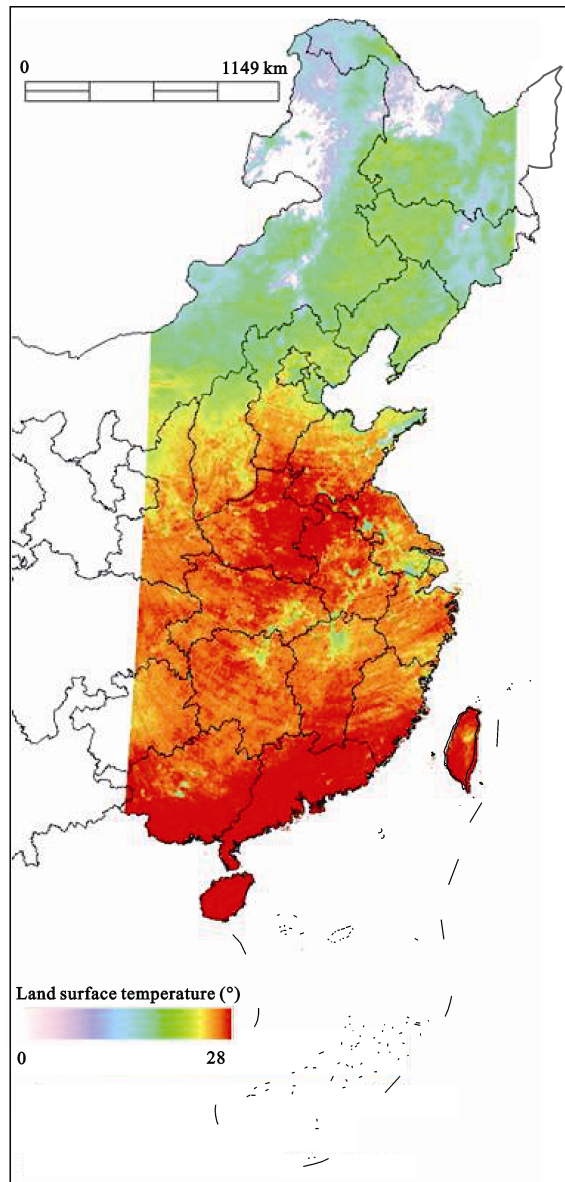


**Fig. 3** Land surface temperature retrieved from the AMSR2 data by using a neural network (NN) (2013.4.13). Blanket area means no data.

that the average accuracy ( $\frac{\sum_{i=1}^n (T_{ri} - T_{gi})}{n}$ ) obtained using the neural network algorithm is approximately  $1.8^\circ$  and that the standard deviation of the retrieval error is approximately  $1.86^\circ$  (shown in Fig. 4). The accuracy is not very stable when the land surface temperature is lower than approximately  $0^\circ$ , and the reason for which is that the radiation situation for soil is different when the temperature of soil is less than  $0^\circ$  (Mao et al., 2007b). We will acquire more field measurements and conduct further comparative analyses in future.

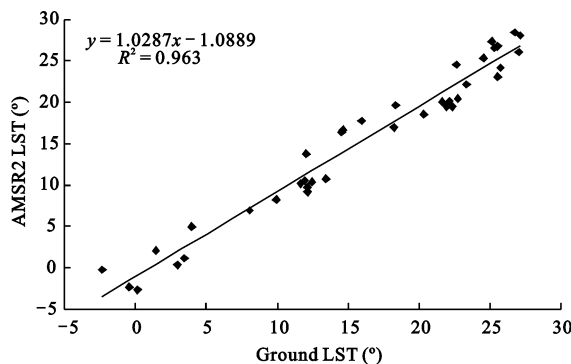


**Fig. 4** Comparison between the LST retrieved from AMSR-E and ground LST measurement

#### 4 Conclusions

On the basis of the radiative transfer equation, we briefly analyzed the ill-posed inversion problem in the retrieval of the land surface temperature from passive microwave data. The emissivity is influenced by the dielectric constant which is a function of the water content, physical temperature, salinity, soil texture and other factors (e.g., the structure and types of vegetation). These factors can make it very difficult to develop a general physical algorithm. An analysis of the relationship between various geophysical parameters indicates that the neural network is one of the best options for retrieving the land surface temperature, as it does not need to know the retrieval rules. The MODIS LST product is set as the land surface data, and a neural network is used to retrieve the land surface temperature from AMSR-E/AMSR2 data. The analysis indicates that the neural network can be used to accurately retrieve land surface temperature from AMSR-E/AMSR2 data. The mean and the standard deviation of the retrieval

error are approximately  $1.4^\circ$  and  $1.9^\circ$  relative to the MODIS LST product when five frequencies (i.e., ten channels) are used. This combination can be employed to eliminate the impacts of the soil moisture, roughness, atmosphere and other influencing factors.

Finally, we utilized the neural network to retrieve the land surface temperature from AMSR2 images over East China. An analysis of the retrieval results indicates that the distribution of the land surface temperature is reasonable. The accuracy was determined to be approximately  $1.8^\circ$  through a comparison of the retrieval results and ground LST measurement data from meteorological stations. We also found that the retrieval error was large in some places. The main reason for this is that there are some lakes in these pixels, which was proven by a terrain map of China. The surface temperature retrieval method for lakes is very different from that for surfaces covered by soil and vegetation because their radiative mechanisms are very different. One suggestion is that a retrieval algorithm should be constructed based on a different training database according to the different ground types and different climates in different regions, especially when the temperature is less than  $0^\circ\text{C}$ . More consideration for mixed pixels should be made in future work.

#### Acknowledgements

The author would like to thank for Ashcroft, P., and F. Wentz. 2003, updated daily. AMSR-E/Aqua L2A Global Swath Spatially-Resampled Brightness Temperatures (Tb) V001, September to October 2003. Boulder, CO, USA: National Snow and Ice Data Center. Digital media, NASA provides MODIS land surface temperature product.

#### References

- Aires F, Prigent C, Rossow W B et al., 2001. A new neural network approach including first guess for retrieval of atmospheric water vapor, cloud liquid water path, surface temperature, and emissivities over land from satellite microwave observations. *Journal of Geophysical Research*, 106(D14): 14887–14907. doi: 10.1029/2001JD900085
- Basist A, Grody N C, Peterson T C et al., 1998. Using the special sensor microwave/imager to monitor land surface temperatures, wetness, and snow cover. *Journal of Applied Meteorology*, 37(9): 888–911. doi: 10.1175/1520-0450(1998)037<0888:UTSSMI>2.0.CO;2

- Becker F, Li Z L, 1990. Towards a local split window method over land surface. *International Journal of Remote Sensing*, 11(3): 369–393. doi: 10.1080/01431169008955028
- Bischof H, Schneider W, Pinz A J, 1992. Multispectral classification of landsat-images using neural networks. *IEEE Transactions on Geoscience and Remote Sensing*, 30(3): 482–489. doi: 10.1109/36.142926
- Blackwell W J, 2005. A neural-network technique for the retrieval of atmospheric temperature and moisture profiles from high spectral resolution sounding data. *IEEE Transactions on Geoscience and Remote Sensing*, 43(11): 2535–2546. doi: 10.1109/TGRS.2005.855071
- Calvet J C, Chanzy A, Wigneron J P, 1996. Surface temperature and soil moisture retrieval in the Sahel from Airborne multi-frequency microwave radiometry. *IEEE Transactions on Geoscience and Remote Sensing*, 34(2): 588–600. doi: 10.1109/36.485135
- Calvet J C, Wigneron J P, Mougin E et al., 1994. Plant water content and temperature of the Amazon forest from satellite microwave radiometry. *IEEE Transactions on Geoscience and Remote Sensing*, 32(2): 397–408. doi: 10.1109/36.295054
- Chen K S, Wu T D, Tsang L et al., 2003. Emission of rough surfaces calculated by the integral equation method with comparison to three-dimensional moment method simulations. *IEEE Transactions on Geoscience and Remote Sensing*, 41(1): 90–101. doi: 10.1109/TGRS.2002.807587
- Chen S S, Chen X Z, Chen W Q et al., 2011. A simple retrieval method of land surface temperature from AMSR-E passive microwave data-A case study over Southern China during the strong snow disaster of 2008. *International Journal of Applied Earth Observation and Geoinformation*, 13(1): 140–151. doi: 10.1016/j.jag.2010.09.007
- Chen Z X, Davis D, Tsang L et al., 1992. Inversion of snow parameters by neural network with iterative inversion. In: *1992 International Geoscience and Remote Sensing Symposium*. Houston, TX: IEEE, 1061–1063. doi: 10.1109/IGARSS.1992.578340
- Choudhury B J, Major E R, Smith E A et al., 1992. Atmospheric effects on SMMR and SSM/I 37 GHz polarization difference over the Sahel. *International Journal of Remote Sensing*, 13(18): 3443–3463. doi: 10.1080/01431169208904133
- Coll C, Caselles V, Sobrino A et al., 1994. On the atmospheric dependence of the split-window equation for land surface temperature. *International Journal of Remote Sensing*, 15(1): 105–122. doi: 10.1080/01431169408954054
- Dash P, Götsche F M, Olesen F S et al., 2002. Land surface temperature and emissivity estimation from passive sensor data: theory and practice-current trends. *International Journal of Remote Sensing*, 23(13): 2563–2594. doi: 10.1080/01431160115041
- Dobson M C, Ulaby F T, Hallikainen M T, 1985. Microwave dielectric behavior of wet soil-part II: dielectric mixing models. *IEEE Transactions on Geoscience and Remote Sensing*, GE-23(1): 35–46. doi: 10.1109/TGRS.1985.289498
- Faure T, Isaka H, Guillemet B, 2001. Neural network retrieval of cloud parameters of inhomogeneous and fractional clouds: feasibility study. *Remote Sensing of Environment*, 77(2): 123–138. doi: 10.1016/S0034-4257(01)00199-7
- Fily M, Royer A, Goïta K et al., 2003. A simple retrieval method for land surface temperature and fraction of water surface determination from satellite microwave brightness temperatures in sub-arctic areas. *Remote Sensing of Environment*, 85(3): 328–338. doi: 10.1016/S0034-4257(03)00011-7
- Gillespie A, Rokugawa S, Matsunaga T et al., 1998. A temperature and emissivity separation algorithm for advanced spaceborne thermal emission and reflection radiometer (ASTER) images. *IEEE Transactions on Geoscience and Remote Sensing*, 36(4): 1113–1126. doi: 10.1109/36.700995
- Givri J R, 1997. The extension of the split window technique to passive microwave surface temperature assessment. *International Journal of Remote Sensing*, 18(2): 335–353. doi: 10.1080/014311697219105
- Hallikainen M T, Ulaby F T, Dobson M C, 1985. Microwave dielectric behavior of wet soil-part 1: empirical models and experimental observations. *IEEE Transactions on Geoscience and Remote Sensing*, GE-23(1): 25–34. doi: 10.1109/TGRS.1985.289497
- Heermann P D, Khazenie N, 1992. Classification of multispectral remote sensing data using a back-propagation neural network. *IEEE Transactions on Geoscience and Remote Sensing*, 30(1): 81–88. doi: 10.1109/36.124218
- Hornik K, Stinchcombe M, White H, 1989. Multilayer feedforward networks are universal approximators. *Neural Network*, 2(5): 359–366. doi: 10.1016/0893-6080(89)90020-8
- Jackson T J, 1997. Soil moisture estimation using special satellite microwave/imager satellite data over a grassland region. *Water Resources Research*, 33(6): 1475–1484. doi: 10.1029/97WR00661
- Jackson T J, O'Neill P E, 1990. Attenuation of soil microwave emission by corn and soybeans at 1.4 and 5 GHz. *IEEE Transactions on Geoscience and Remote Sensing*, 28(5): 978–980. doi: 10.1109/36.58989
- Jackson T J, Schmugge T J, 1991. Vegetation effects on the microwave emission from soils. *Remote Sensing of Environment*, 36(3): 203–212. doi: 10.1016/0034-4257(91)90057-D
- Jackson T J, Schmugge T J, Wang J R, 1982. Passive microwave remote sensing of soil moisture under vegetation canopies. *Water Resources Research*, 18(4): 1137–1142. doi: 10.1029/WR018i004p01137
- Jin Y Q, Liu C, 1997. Biomass retrieval from high-dimensional active/passive remote sensing data by using artificial neural networks. *International Journal of Remote Sensing*, 18(4): 971–979. doi: 10.1080/014311697218863
- Kerr Y H, Lagouarde J P, Imbernon J, 1992. Accurate land surface temperature retrieval from AVHRR data with use of an improved split window algorithm. *Remote Sensing of Environment*, 41(2–3): 197–209. doi: 10.1016/0034-4257(92)90078-X
- Kerr Y H, Njoku E G, 1990. A semiempirical model for interpreting microwave emission from semiarid land surfaces as seen from space. *IEEE Transactions on Geoscience and Re-*

- mote Sensing*, 28(3): 384–393. doi: 10.1109/36.54364
- Kerr Y H, Njoku E G, 1993. On the use of passive microwaves at 37 GHz in remote sensing of vegetation. *International Journal of Remote Sensing*, 14(10): 1931–1943. doi: 10.1080/01431169308954013
- Liang S L, 2001. An optimization algorithm for separating land surface temperature and emissivity from multispectral thermal infrared imagery. *IEEE Transactions on Geoscience and Remote Sensing*, 39(2): 264–274. doi: 10.1109/36.905234
- Mao K B, Shi J C, Li Z L et al., 2007a. An RM-NN algorithm for retrieving land surface temperature and emissivity from EOS/MODIS data. *Journal of Geophysical Research*, 112(D21): D21102, doi: 10.1029/2007JD008428
- Mao K B, Shi J C, Tang H J et al., 2007c. A neural-network technique for retrieving land surface temperature from AMSR-E passive microwave data. In: *2007 IEEE International Geoscience and Remote Sensing Symposium*. Barcelona: IEEE, 4422–4425. doi: 10.1109/IGARSS.2007.4423835
- Mao K B, Shi J C, Tang H J et al., 2008. A neural network technique for separating land surface emissivity and temperature from ASTER imagery. *IEEE Transactions on Geoscience and Remote Sensing*, 46(1): 200–208. doi: 10.1109/TGRS.2007.907333
- Mao K, Qin Z, Shi J et al., 2005. A practical split-window algorithm for retrieving land-surface temperature from MODIS data. *International Journal of Remote Sensing*, 26(15): 3181–3204. doi: 10.1080/01431160500044713
- Mao Kebiao, Shi Jiancheng, Li Zhaoliang et al., 2007b. A physics-based statistical algorithm for retrieving land surface temperature from AMSR-E passive microwave data. *Science in China Series D: Earth Sciences*, 50(7): 1115–1120. doi: 10.1007/s11430-007-2053-x
- McFarland M J, Miller R L, Neale C M U, 1990. Land surface temperature derived from the SSM/I passive microwave brightness temperatures. *IEEE Transactions on Geoscience and Remote Sensing*, 28(5): 839–845. doi: 10.1109/36.58971
- Morland J C, Grimes D I F, Hewison T J, 2001. Satellite observations of the microwave emissivity of a semi-arid land surface. *Remote Sensing of Environment*, 77(2): 149–164. doi: 10.1016/S0034-4257(01)00202-4
- Njoku E G, Ashcroft P, Chan T K et al., 2005. Global survey and statistics of radio-frequency interference in AMSR-E land observations. *IEEE Transactions on Geoscience and Remote Sensing*, 43(5): 938–947. doi: 10.1109/TGRS.2004.837507
- Njoku E G, Chan S K, 2006. Vegetation and surface roughness effects on AMSR-E land observations. *Remote Sensing of Environment*, 100(2): 190–199. doi: 10.1016/j.rse.2005.10.017
- Njoku E G, Jackson T J, Lakshmi V et al., 2003. Soil moisture retrieval from AMSR-E. *IEEE Transactions on Geoscience and Remote Sensing*, 41(2): 215–229. doi: 10.1109/TGRS.2002.808243
- Njoku E G, Li L, 1999. Retrieval of land surface parameters using passive microwave measurements at 6–18GHz. *IEEE Transactions on Geoscience and Remote Sensing*, 37(1): 79–93. doi: 10.1109/36.739125
- Owe M, de Jeu R, Walker J, 2001. A methodology for surface soil moisture and vegetation optical depth retrieval using the microwave polarization difference index. *IEEE Transactions on Geoscience and Remote Sensing*, 39(8): 1643–1654. doi: 10.1109/36.942542
- Paloscia S, Pampaloni, 1988. Microwave polarization index for monitoring vegetation growth. *IEEE Transactions on Geoscience and Remote Sensing*, 26(5): 617–621. doi: 10.1109/36.7687
- Prata A J, 1994. Land surface temperatures derived from the advanced very high resolution radiometer and the along-track scanning radiometer: 2. Experimental results and validation of AVHRR algorithms. *Journal of Geophysical Research*, 99(D6): 13025–13058. doi: 10.1029/94JD00409
- Price J C, 1984. Land surface temperature measurements from the split window channels of the NOAA 7 advanced very high resolution radiometer. *Journal of Geophysical Research*, 89(D5): 7231–7237. doi: 10.1029/JD089iD05p07231
- Prigent C, Aires F, Rossow W B, 2003. Land surface skin temperatures from a combined analysis of microwave and infrared satellite observations for an all-weather evaluation of the differences between air and skin temperatures. *Journal of Geophysical Research*, 108(D10): 4310, doi: 10.1029/2002JD002301
- Pulliainen J T, Grandell J, Hallikainen M T, 1997. Retrieval of surface temperature in Boreal Forest Zone from SSM/I data. *IEEE Transactions on Geoscience and Remote Sensing*, 35(5): 1188–1200. doi: 10.1109/36.628786
- Shi J C, Jiang L M, Zhang L X et al., 2005. A parameterized multifrequency-polarization surface emission model. *IEEE Transactions on Geoscience and Remote Sensing*, 43(12): 2831–2841. doi: 10.1109/TGRS.2005.857902
- Sobrino J A, Coll C, Caselles V, 1991. Atmospheric correction for land surface temperature using NOAA-11 AVHRR channels 4 and 5. *Remote Sensing of Environment*, 38(1): 19–34. doi: 10.1016/0034-4257(91)90069-I
- Susskind J, Rosenfield J, Reuter D et al., 1984. Remote sensing of weather and climate parameters from HIRS2/MSU on Tiros-N. *Journal of Geophysical Research*, 89(D3): 4677–4697. doi: 10.1029/JD089iD03p04677
- Tang L, Chen Z, Oh S et al., 1992. Inversion of snow parameters from passive microwave remote sensing measurements by a neural network trained with a multiple scattering model. *IEEE Transactions on Geoscience and Remote Sensing*, 30(5): 1015–1024. doi: 10.1109/36.175336
- Tedesco M, Pulliainen J, Takala M et al., 2004. Artificial neural network-based techniques for the retrieval of SWE and snow depth from SSM/I data. *Remote Sensing of Environment*, 90(1): 76–85. doi: 10.1016/j.rse.2003.12.002
- Tzeng Y C, Chen K S, Kao W L et al., 1994. A Dynamic learning neural network for remote sensing applications. *IEEE Transactions on Geoscience and Remote Sensing*, 32(5): 1096–1102. doi: 10.1109/36.312898
- Wan Z M, Dozier J, 1996. A generalized split-window algorithm for retrieving land-surface temperature from space. *IEEE Transactions on Geoscience and Remote Sensing*, 34(4):

- 892–905. doi: 10.1109/36.508406
- Wan Z M, Zhang Y L, Zhang Q C et al., 2002. Validation of the land-surface temperature products retrieved from Terra Moderate Resolution Imaging Spectroradiometer data. *Remote Sensing of Environment*, 83(1–2): 163–180. doi: 10.1016/S 0034-4257(02)00093-7
- Wan Z, Zhang Y, Zhang Q et al., 2004. Quality assessment and validation of the MODIS global land surface temperature. *International Journal of Remote Sensing*, 25: 261–274. doi: 10.1080/0143116031000116417.
- Weng F Z, Grody N C, 1998. Physical retrieval of land surface temperature using the special sensor microwave imager. *Journal of Geophysical Research*, 103(D8): 8839–8848. doi: 10.1029/98JD00275
- Wu T D, Chen K S, Shi J C et al., 2001. A transition model for the reflection coefficient in surface scattering. *IEEE Transactions on Geoscience and Remote Sensing*, 39(9): 2040–2050. doi: 10.1109/36.951094
- Xia L, Mao K B, Ma Y et al., 2014. An algorithm for retrieving land surface temperatures using VIIRS data in combination with multi-sensors. *Sensors*, 14(11): 21385–21408. doi: 10.3390/s141121385